Spiral magnetic structure in spin-$\frac{5}{2}$ frustrated trimerized chains in $SrMn_3P_4O_{14}$

Masashi Hase,[1,*] Vladimir Yu. Pomjakushin,[2] Lukas Keller,[2] Andreas Dönni,[1] Osamu Sakai,[1] Tao Yang,[3] Rihong Cong,[3] Jianhua Lin,[3] Kiyoshi Ozawa,[1] and Hideaki Kitazawa[1]

[1]*National Institute for Materials Science (NIMS), 1-2-1 Sengen, Tsukuba, Ibaraki 305-0047, Japan*

[2]*Laboratory for Neutron Scattering, Paul Scherrer Institut (PSI), CH-5232 Villigen PSI, Switzerland*

[3]*College of Chemistry and Molecular Engineering, Peking University, Beijing 100871, People's Republic of China*

(Received 1 November 2011; revised manuscript received 16 November 2011; published 29 November 2011)

We study a spin-5/2 antiferromagnetic trimerized chain substance $SrMn_3P_4O_{14}$ using neutron powder diffraction experiments. The coplanar spiral magnetic structure appears below $T_{N1} = 2.2(1)$ K. Values of several magnetic structure parameters change rapidly at $T_{N2} = 1.75(5)$ K, indicating another phase transition, although the magnetic structures above and below T_{N2} are qualitatively the same. The spiral magnetic structure can be explained by frustration between nearest-neighbor and next-nearest-neighbor exchange interactions in the trimerized chains.

DOI: 10.1103/PhysRevB.84.184435 PACS number(s): 75.25.−j, 75.10.Jm, 75.30.Kz, 75.40.Cx

I. INTRODUCTION

Frustrated magnets can exhibit intriguing magnetic states such as the quantum spin-liquid state,[1] the chiral ordered state,[2,3] the spin nematic or the multipolar state,[4,5] and the spin-gel state.[6] Therefore, frustrated magnets have been investigated extensively. Among various frustrated magnets, frustrated spin chains provide ideal grounds for studies.[7,8] Frustrated spin chains are simple models that still show surprisingly rich physics. For example, in the frustrated spin-1/2 chain with ferromagnetic nearest-neighbor and antiferromagnetic next-nearest-neighbor exchange interactions (J_{NN} and J_{NNN} interactions, respectively) in the presence of magnetic fields, theoretical studies predict various ground-state phases including the vector chiral phase, the nematic phase, other multipolar phases, and the spin-density-wave phases.[9–18] Several model substances have been found and are summarized in Table 1 in Ref. [19] or Fig. 5 in Ref. [20]. Experimental results are compared with theoretical results.[14,18]

Theoretical investigations were performed in frustrated longer-period spin chains such as alternating chains,[21–24] while there is almost no model substance. To our knowledge, the only example is $CuGeO_3$. The frustrated alternating spin-1/2 chain is realized in the spin-Peierls state.[25–32] In most of the one-dimensional (1D) magnets, the spin-spin distance in the J_{NNN} interaction is large. Therefore the J_{NNN} interaction is usually much smaller than the J_{NN} interaction. It is difficult to find model substances having frustrated spin chains.

We have focused on $SrMn_3P_4O_{14}$. We expected the $J_1 - J_1 - J_2$ trimerized chain shown in Fig. 1.[33] The magnetization results could be explained using the spin-5/2 trimer formed by the antiferromagnetic (AF) J_1 interaction ($J_1/k = 4.0$ K).[34] Magnetic excitations were observed in inelastic neutron scattering experiments and could be also explained using the trimer model.[35] Therefore the J_2 value is small in comparison with the J_1 value. A magnetic phase transition appears at about 2.6 K.[33] Therefore the J_2 interaction is not negligible. The J_2 interaction may be comparable to NNN exchange interactions in the chain. We expected the occurrence of an unconventional magnetic structure and performed neutron powder diffraction experiments. In this paper we report that $SrMn_3P_4O_{14}$ shows a coplanar spiral magnetic structure. In the classical limit the ground state of the frustrated uniform spin chain has a spiral magnetic structure with a pitch angle $\cos^{-1}(-J_{NN}/4J_{NNN})$ for $|J_{NN}/J_{NNN}| < 4$.[36] Similarly, we can explain the spiral magnetic structure in $SrMn_3P_4O_{14}$ by taking the J_1, J_2, and NNN exchange interactions in the chain into account.

II. EXPERIMENT

We synthesized $SrMn_3P_4O_{14}$ powders under hydrothermal conditions.[33] We carried out neutron powder diffraction experiments at the Swiss spallation neutron source SINQ at the Paul Scherrer Institute. We used the high-resolution powder diffractometer for thermal neutrons HRPT (wavelength $\lambda = 1.886$ Å, high-intensity mode $\Delta d/d \geqslant 1.8 \times 10^{-3}$),[37] and the high-intensity cold neutron powder diffractometer (DMC) with $\lambda = 2.458$ Å. We performed Rietveld refinements of crystal and magnetic structures using the FULLPROF SUITE program package,[38] with the use of its internal tables for scattering lengths and magnetic form factors.

III. RESULTS

Figure 2 depicts the neutron powder diffraction pattern of $SrMn_3P_4O_{14}$ recorded using the HRPT diffractometer with $\lambda = 1.886$ Å at 4.0 K (paramagnetic state). The crystal structure model in the space group $P2_1/c$ (no. 14) proposed in [33] fits our data well. The refined structure parameters are presented in Table I. They were kept fixed in the subsequent refinements of the magnetic structure.

Figure 3 depicts fragments of diffraction patterns recorded using the DMC diffractometer. We observed many new reflections below $T_{N1} = 2.2(1)$ K. One of them is shown in Fig. 3(a). The magnetic susceptibility data indicate a magnetic phase transition at low T.[33] Therefore the new reflections are magnetic reflections. The position of the reflection in Fig. 3(a) is shifted clearly and the intensity increases rapidly between 1.7 and 1.8 K, indicating another phase transition. Diffuse scattering is readily apparent in Fig. 3(b). Several magnetic reflections exist between 20° and 35° below T_{N1}. Therefore, the diffuse scattering stems from magnetic correlations. The shape of the diffuse scattering resembles one- or two-dimensional magnetic Bragg scattering with a cutoff at low Q and long tail

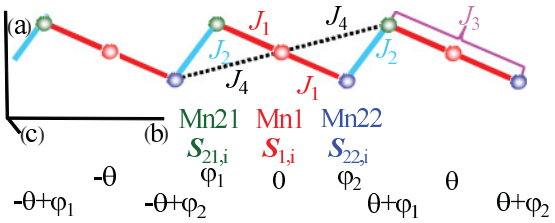

FIG. 1. (Color online) The spin system in $SrMn_3P_4O_{14}$. Mn^{2+} ions ($3d^5$) have localized spin 5/2. Two kinds of short Mn–Mn bonds exist. The Mn–Mn distances are 3.26 and 3.31 Å at 4.0 K. The exchange interaction parameters are respectively defined as J_1 and J_2. The J_1 and J_2 interactions form a trimerized chain that is almost parallel to the b axis. The value of the antiferromagnetic J_1 interaction was evaluated as 3.4–4.0 K (Refs. 34 and 35). The J_3 and J_4 interactions are the next-nearest-neighbor exchange interactions in the chain. $\mathbf{S}_{1,i}$, $\mathbf{S}_{21,i}$, and $\mathbf{S}_{22,i}$ are spin operators. We use the parameters θ, φ_1, and φ_2 to show angles between magnetic moments in a coplanar spiral magnetic structure.

at high Q (scattering vector magnitude). As the temperature T is lowered, the intensity around 25° increases down to 2.6 K and decreases below 2.6 K. The diffuse scattering remains even at 1.5 K.

The circles in Fig. 4 represent the neutron powder diffraction pattern at 1.5 K recorded using the DMC diffractometer. The magnetic reflections can all be indexed with a propagation vector $\mathbf{k} = [0, k_y, 0]$ with $k_y \sim 0.32$. Using the determined propagation vector we performed the symmetry analysis according to Izyumov *et al.*[39] to derive possible magnetic configurations for Mn1 (2*d*) and Mn2 (4*e*) sites. For the calculation of the basis functions we used the BASIREP program.[38] The little group of a propagation vector for the space group $P2_1/c$ contains only two symmetry operators, 1 and $\{2_y|0\frac{1}{2}\frac{1}{2}\}$, resulting in the splitting of Mn2 (4*e*) into two independent orbits, Mn21 and Mn22 sites. The little group has two 1D irreducible representations (IRs) τ_1 and τ_2 with the characters for 2_y: $\pm e^{-i\pi k_y}$, respectively. Both IRs enter three times the magnetic representation for all three Mn sites. The basis functions for τ_2 dictate the absence of the $(0,1-k,0)$ magnetic reflection, which indeed has zero intensity. Therefore we can

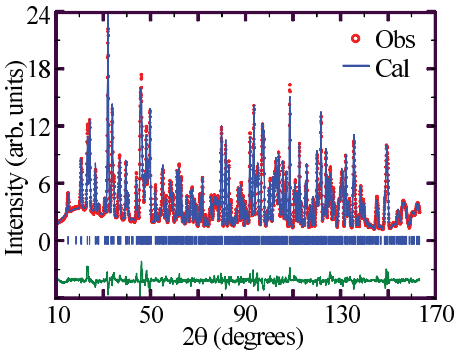

FIG. 2. (Color online) Neutron powder diffraction pattern of $SrMn_3P_4O_{14}$ at 4.0 K measured using the HRPT diffractometer ($\lambda = 1.886$ Å). Lines on the observed pattern and at the bottom show a Rietveld refined pattern and the difference between the observed and the Rietveld refined patterns, respectively. Hash marks represent the positions of nuclear reflections.

TABLE I. Structural parameters of $SrMn_3P_4O_{14}$ derived from Rietveld refinement of the HRPT neutron powder diffraction pattern at 4.0 K. The space group is monoclinic $P2_1/c$ (no. 14). The lattice constants at 4.0 K are $a = 7.661(1)$ Å, $b = 7.784(1)$ Å, $c = 9.638(1)$ Å, and $\beta = 111.70(2)°$. Estimated standard deviations are shown in parentheses. We constrained the atomic displacement parameters B_{iso} at 4.0 K of two Mn sites to be the same and those of two P sites to be the same. We took absorption effects into account. The reliability factors of the refinement are $R_{wp} = 5.10\%$, $R_{exp} = 1.53\%$, $\chi^2 = 11.2$, and $R_{Bragg} = 4.04\%$. The values of B_{iso} at 4.0 K may be small. To obtain more precise values of B_{iso}, we measured a diffraction pattern at 290 K using neutrons with the shorter wavelength (1.494 Å) and performed Rietveld refinements. The values of B_{iso} at 290 K are shown in this table. They are not small. Atomic positions at 290 K are the same as those at 4.0 K within experimental error.

					B_{iso} Å^2	
Atom	Site	x	y	z	4.0 K	290 K
Sr	2*a*	0	0	0	0.15(5)	0.72(5)
Mn1	2*b*	0.5	0	0	0.17(5)	0.15(8)
Mn2	4*e*	0.6895(5)	0.1193(5)	0.5332(4)	0.17(5)	0.68(6)
P1	4*e*	0.6186(4)	0.7051(4)	0.8061(3)	0.29(4)	0.67(5)
P2	4*e*	0.8937(4)	0.0600(3)	0.2966(3)	0.29(4)	0.39(5)
O1	4*e*	0.1228(3)	0.6832(3)	0.0903(3)	0.12(4)	0.67(4)
O2	4*e*	0.3326(3)	0.1255(3)	0.1123(3)	0.21(4)	0.63(4)
O3	4*e*	0.8187(3)	0.8764(3)	0.3219(3)	0.18(4)	0.72(4)
O4	4*e*	0.4650(3)	0.0820(3)	0.6128(2)	0.09(4)	0.47(4)
O5	4*e*	0.7694(3)	0.1162(3)	0.1351(2)	0.28(4)	0.65(4)
O6	4*e*	0.5100(3)	0.7143(3)	0.6411(3)	0.04(4)	0.59(4)
O7	4*e*	0.0910(3)	0.0213(3)	0.2991(3)	0.22(4)	0.64(4)

immediately choose τ_2. Nevertheless, we have performed a simulated annealing search of the magnetic structures for both IRs. The τ_2 produced excellent results, although the τ_1 failed. We found that the y components of magnetic moments can be ignored and performed final refinements under the following conditions. Only the x and z components of magnetic moments are considered. The Mn21 and Mn22 sites

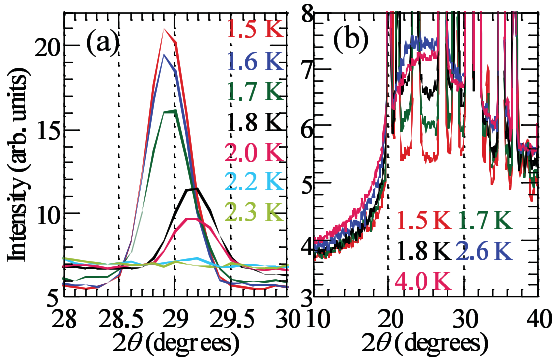

FIG. 3. (Color online) Neutron powder diffraction patterns of $SrMn_3P_4O_{14}$ measured using the DMC diffractometer ($\lambda = 2.458$ Å). The temperature T of each curve is understood from the following T dependence. (a) The peak intensity decreases monotonically with increasing T. (b) The intensity at 25° is smallest at 1.5 K. As T is raised, the intensity at 25° increases and is largest at 2.6 K. The pattern at 4.0 K is positioned just below the 2.6 K pattern.

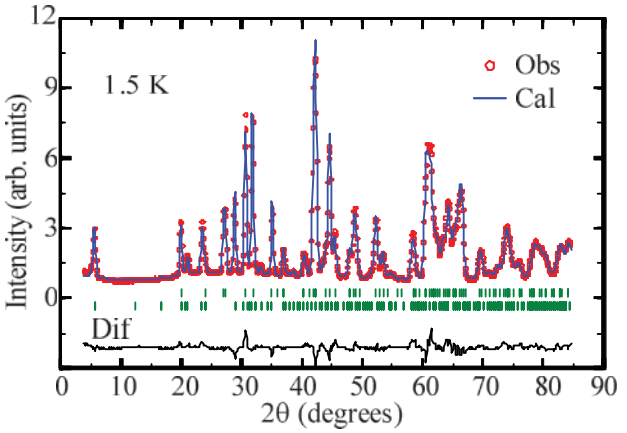

FIG. 4. (Color online) Neutron powder diffraction pattern of $SrMn_3P_4O_{14}$ at 1.5 K measured using the DMC diffractometer ($\lambda = 2.458$ Å). Lines on the observed pattern and at the bottom show a Rietveld refined pattern and the difference between the observed and the Rietveld refined patterns, respectively. Upper and lower hash marks represent the positions of nuclear and magnetic reflections, respectively.

are crystallographically identical. Therefore the magnitudes of Mn21 and Mn22 moments are constrained as identical. In general, the magnetic structure consists of ellipsoidal spirals running on all three Mn sites with independent phases. The spin 5/2 of Mn^{2+} ions is almost isotropic.[34] Therefore we assumed a circular spiral magnetic structure.

The line on the observed pattern at 1.5 K in Fig. 4 shows a Rietveld refined pattern including both nuclear and magnetic contributions. It can well reproduce the observed pattern. Figure 5 depicts the coplanar spiral magnetic structure at 1.5 K. The value of k_y is 0.317, indicating an incommensurate magnetic structure. Magnetic moments have x and z components. The angle between Mn1 and Mn21 (Mn22) moments in each trimer is 166(4)° [164(4)°]. The angle between Mn21 and Mn22 moments in the J_2 bond is 111(3)°. These angles indicate that both the J_1 and J_2 interactions are AF.

Figure 6 shows the T dependence of several magnetic structure parameters. The value of k_y changes abruptly

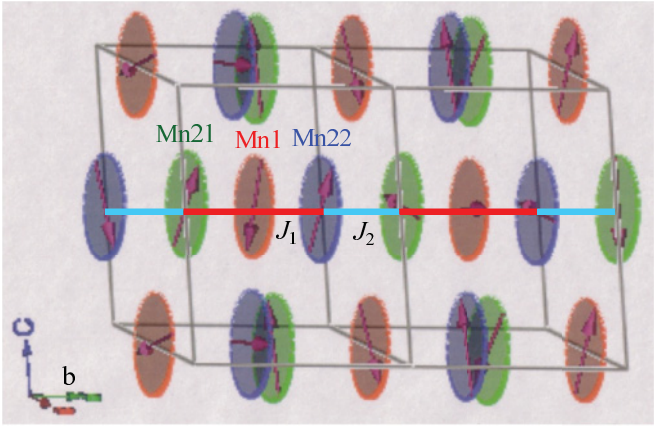

FIG. 5. (Color online) The coplanar spiral magnetic structure of $SrMn_3P_4O_{14}$ at 1.5 K.

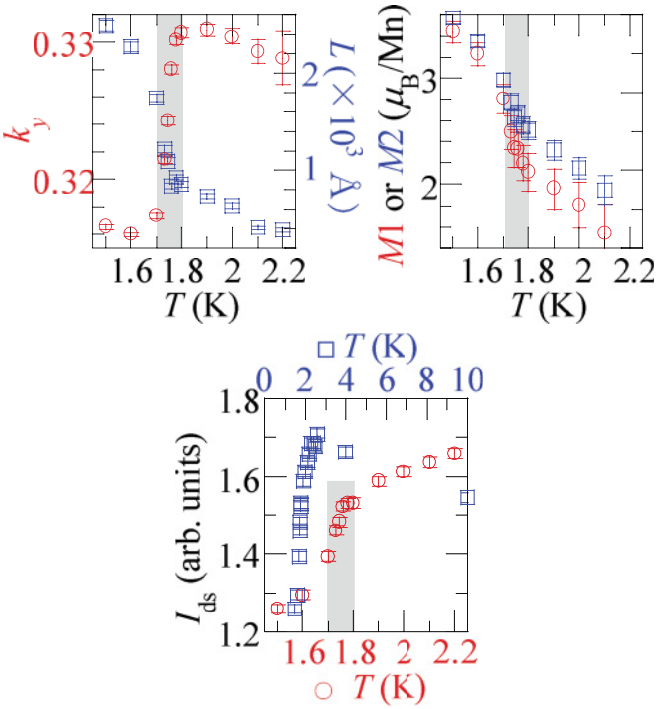

FIG. 6. (Color online) Temperature dependence of several magnetic structure parameters of $SrMn_3P_4O_{14}$. Circles and squares in (a) show the y component of the propagation vector (the left vertical axis) and the size of magnetic domains (right), respectively. Circles and squares in (b) show the magnitudes of the magnetic moments of Mn1 and Mn2, respectively. Integrated intensities of the diffuse magnetic scattering (plus backgrounds) between 24.4 and 26.7° are shown as circles (lower horizontal scale) and squares (upper) in (c). The hatched area shows the transition region around T_{N2}.

between 1.7 and 1.8 K, indicating another phase transition at $T_{N2} = 1.75(5)$ K. As T is lowered, the magnitudes of the Mn1 and Mn2 moments ($M1$ and $M2$) increase. The size of magnetic domains L was determined from Lorentzian broadening of the magnetic reflections. The value of L increases concomitantly with decreasing T. Figure 6(c) shows the integrated intensity I_{ds} between $2\theta = 24.4°$ and 26.7°, where diffuse scattering is apparent, as presented in Fig. 3(b). As T is lowered below T_{N1}, the value of I_{ds} decreases, indicating that the diffuse scattering is weakened. We emphasize that $M1$, $M2$, L, and I_{ds} change rapidly at around $T_{N2} = 1.75(5)$ K.

IV. DISCUSSION

We discuss the origin of the spiral magnetic structure in $SrMn_3P_4O_{14}$. Most spiral magnetic structures are caused by magnetic frustration among plural symmetric exchange interactions. As described in Sec. I, magnetic frustration between NN and NNN exchange interactions in a uniform spin chain can generate a spiral magnetic structure.[36] We consider whether magnetic frustration between NN and NNN exchange interactions in a trimerized spin chain can generate a spiral magnetic structure or not. The two kinds of NNN exchange interactions (J_3 and J_4) may exist (Fig. 1).

The Hamiltonian of the exchange interactions is given as follows:

$$\begin{aligned}\mathcal{H}_{\rm ex} = \Sigma_i\{&J_1(\mathbf{S}_{1,i}\cdot\mathbf{S}_{21,i}+\mathbf{S}_{1,i}\cdot\mathbf{S}_{22,i})\\&+J_2\mathbf{S}_{21,i}\cdot\mathbf{S}_{22,i-1}+J_3\mathbf{S}_{21,i}\cdot\mathbf{S}_{22,i}\\&+J_4(\mathbf{S}_{1,i}\cdot\mathbf{S}_{21,i+1}+\mathbf{S}_{1,i}\cdot\mathbf{S}_{22,i-1})\}.\end{aligned}\quad(1)$$

According to the experimental results, we restrict classical ground states of this Hamiltonian to states in which magnetic moments lie in the ac plane. The relative angle of each magnetic moment from the central Mn1 moment in Fig. 1 can be defined by one parameter such as $-\theta+\varphi_1$, $-\theta$, and so on. The classical exchange energy per trimer is expressed as follows:

$$\begin{aligned}E_{\rm ex} = (g\mu_{\rm B})^{-2}[&J_1M_1M_2(\cos\varphi_1+\cos\varphi_2)\\&+J_2M_2M_2\cos(\theta+\varphi_1-\varphi_2)\\&+J_3M_2M_2\cos(\varphi_1-\varphi_2)\\&+J_4M_1M_2\{\cos(\theta+\varphi_1)+\cos(\theta-\varphi_2)\}].\end{aligned}\quad(2)$$

We examine whether we can reproduce the experimental values of θ, 114° and 119° at 1.5 K and 1.8 K, respectively, under the condition that the experimental values of φ_1, φ_2, and $M_1/M_2\equiv\alpha$ are given. The experimental values of φ_1, φ_2, and α are, respectively, 166(4)°, 164(4)°, and 0.96 at 1.5 K, and 170(4)°, 160(4)°, and 0.84 at 1.8 K. The θ-dependent part of the classical exchange energy $E'(\theta)$ is given in Eq. (3):

$$\begin{aligned}\frac{E'(\theta)_{\rm ex}(g\mu_{\rm B})^2}{J_2M_2^2} = &\cos(\theta+\varphi_1-\varphi_2)+j_4\alpha\{\cos(\theta+\varphi_1)\\&+\cos(\theta-\varphi_2)\}.\end{aligned}\quad(3)$$

The classical exchange energy shows a minimum at $\theta=114°$ when $J_4/J_2\equiv j_4=0.53$ and $\theta=119°$ when $j_4=0.58$. Consequently, the coplanar spiral magnetic structure in $SrMn_3P_4O_{14}$ can be explained by the frustration between the NN and NNN exchange interactions in the chains. We speculate that the value of j_4 is changed at $T_{\rm N2}$ by a structural phase transition which we have not detected. The value of k_y at 1.8 K is close to 1/3. We cannot determine whether the magnetic structure above $T_{\rm N2}$ is commensurate or not. In the frustrated trimerized chain model, it is not important whether it is commensurate or not. The following problems should be solved in further investigations. $E_{\rm ex}$ is unchanged when we exchange φ_1 and $-\varphi_2$. $E_{\rm ex}$ can be a minimum when $\varphi_1=-\varphi_2$. Therefore, we cannot deduce the experimental values of φ_1 and φ_2 from this model. In addition, this model cannot explain why the coplanar magnetic structure appears. We should consider anisotropy.

We describe another origin of spiral magnetic structures. Competition between symmetric exchange and Dzyaloshinskii-Moriya (DM) interactions can produce spiral magnetic structures. Examples of materials are $Ba_2CuGe_2O_7$,[40] $CsCuCl_3$,[41] and CuB_2O_4.[42] A uniform component of DM vectors is necessary. In $SrMn_3P_4O_{14}$, the J_1 interaction is dominant. The DM interaction between Mn1 and Mn2 spins in the J_1 bond may exist because of the symmetry. The Mn1 site is an inversion center. The DM vector between Mn1 and Mn21 spins is antiparallel to the DM vector between Mn1 and Mn22 spins, i.e., the DM vectors have no uniform component. Accordingly, the DM interaction in the J_1 bond cannot be the origin of the spiral magnetic structure in $SrMn_3P_4O_{14}$. The J_2 interaction is probably the second dominant. The DM interaction between Mn21 and Mn22 spins in the J_2 bond cannot exist because of the symmetry.

V. CONCLUSION

We performed neutron powder diffraction experiments on the spin-5/2 antiferromagnetic trimerized chain substance $SrMn_3P_4O_{14}$. The coplanar spiral magnetic structure appears below $T_{\rm N1}=2.2(1)$ K. The propagation vector is parallel to the y axis with a typical y component of 0.3. The magnetic moments lie in the ac plane in the monoclinic crystal structure. The magnetic diffuse scattering is apparent at low temperatures and remains even at 1.5 K. The shape of the diffuse scattering resembles one- or two-dimensional magnetic Bragg scattering with a cutoff at low Q and long tail at high Q (scattering vector magnitude). Values of several magnetic structure parameters change rapidly at $T_{\rm N2}=1.75(5)$ K, indicating another phase transition, although the magnetic structures above and below $T_{\rm N2}$ are the qualitatively same. The spiral magnetic structure can be explained by the frustration between the nearest-neighbor and next-nearest-neighbor exchange interactions in the trimerized chains.

ACKNOWLEDGMENTS

This work was partially supported by grants from NIMS. The neutron powder diffraction experiments were conducted at SINQ, PSI Villigen, Switzerland. We are grateful to T. Masuda, T. Arima, M. Kohno, and H. Sakurai for invaluable discussion.

*hase.masashi@nims.go.jp

[1] P. W. Anderson, Mater. Res. Bull. **8**, 153 (1973).
[2] S. Miyashita and H. Shiba, J. Phys. Soc. Jpn. **53**, 1145 (1984).
[3] S. Onoda and N. Nagaosa, Phys. Rev. Lett. **99**, 027206 (2007).
[4] H. Tsunetsugu and M. Arikawa, J. Phys. Soc. Jpn. **75**, 083701 (2006).
[5] M. E. Zhitomirsky, Phys. Rev. B **78**, 094423 (2008).
[6] H. Kawamura, A. Yamamoto, and T. Okubo, J. Phys. Soc. Jpn. **79**, 023701 (2010).
[7] F. D. M. Haldane, Phys. Rev. B **25**, 4925 (1982).
[8] F. D. M. Haldane, Phys. Rev. B **26**, 5257 (1982).
[9] A. V. Chubukov, Phys. Rev. B **44**, 4693 (1991).
[10] A. Kolezhuk and T. Vekua, Phys. Rev. B **72**, 094424 (2005).
[11] F. Heidrich-Meisner, A. Honecker, and T. Vekua, Phys. Rev. B **74**, 020403(R) (2006).
[12] T. Vekua, A. Honecker, H.-J. Mikeska, and F. Heidrich-Meisner, Phys. Rev. B **76**, 174420 (2007).
[13] L. Kecke, T. Momoi, and A. Furusaki, Phys. Rev. B **76**, 060407(R) (2007).
[14] T. Hikihara, L. Kecke, T. Momoi, and A. Furusaki, Phys. Rev. B **78**, 144404 (2008).

[15]J. Sudan, A. Luscher, and A. M. Läuchli, Phys. Rev. B **80**, 140402(R) (2009).
[16]M. Sato, T. Momoi, and A. Furusaki, Phys. Rev. B **79**, 060406(R) (2009).
[17]F. Heidrich-Meisner, I. P. McCulloch, and A. K. Kolezhuk, Phys. Rev. B **80**, 144417 (2009).
[18]M. Sato, T. Hikihara, and T. Momoi, Phys. Rev. B **83**, 064405 (2011).
[19]M. Hase, H. Kuroe, K. Ozawa, O. Suzuki, H. Kitazawa, G. Kido, and T. Sekine, Phys. Rev. B **70**, 104426 (2004).
[20]S.-L. Drechsler, O. Volkova, A. N. Vasiliev, N. Tristan, J. Richter, M. Schmitt, H. Rosner, J. Málek, R. Klingeler, A. A. Zvyagin, and B. Büchner, Phys. Rev. Lett. **98**, 077202 (2007).
[21]S. Brehmer, H.-J. Mikeska, and U. Neugebauer, J. Phys.: Condens. Matter **8**, 7161 (1996).
[22]T. Nakamura, S. Takada, K. Okamoto, and N. Kurosawa, J. Phys. Condens. Matter **9**, 6401 (1997).
[23]S. Brehmer, A. K. Kolezhuky, H.-J. Mikeska, and U. Neugebauer, J. Phys.: Condens. Matter **10**, 1103 (1998).
[24]S. Watanabe and H. Yokoyama, J. Phys. Soc. Jpn. **68**, 2073 (1999).
[25]M. Hase, I. Terasaki, and K. Uchinokura, Phys. Rev. Lett. **70**, 3651 (1993).
[26]M. Hase, I. Terasaki, Y. Sasago, K. Uchinokura, and H. Obara, Phys. Rev. Lett. **71**, 4059 (1993).
[27]M. Hase, I. Terasaki, K. Uchinokura, M. Tokunaga, N. Miura, and H. Obara, Phys. Rev. B **48**, 9616 (1993).
[28]M. Hase, N. Koide, K. Manabe, Y. Sasago, K. Uchinokura, and A. Sawa, Physica B **215**, 164 (1995).
[29]G. Castilla, S. Chakravarty, and V. J. Emery, Phys. Rev. Lett. **75**, 1823 (1995).
[30]J. Riera and A. Dobry, Phys. Rev. B **51**, 16098 (1995).
[31]M. Hase, K. Uchinokura, R. J. Birgeneau, K. Hirota, and G. Shirane, J. Phys. Soc. Jpn. **65**, 1392 (1996).
[32]M. C. Martin, M. Hase, K. Hirota, G. Shirane, Y. Sasago, N. Koide, and K. Uchinokura, Phys. Rev. B **56**, 3173 (1997).
[33]T. Yang, Y. Zhang, S. Yang, G. Li, M. Xiong, F. Liao, and J. Lin, Inorg. Chem. **47**, 2562 (2008).
[34]M. Hase, T. Yang, R. Cong, J. Lin, A. Matsuo, K. Kindo, K. Ozawa, and H. Kitazawa, Phys. Rev. B **80**, 054402 (2009).
[35]M. Hase, M. Matsuda, K. Kaneko, N. Metoki, K. Kakurai, T. Yang, R. Cong, J. Lin, K. Ozawa, and H. Kitazawa, e-print arXiv:1109.6720 [cond-mat] (to be published).
[36]R. Bursil, G. A. Gehring, D. J. J. Farnell, J. B. Parkinson, T. Xiang, and C. Zeng, J. Phys.: Condens. Matter **7**, 8605 (1995).
[37]P. Fischer, G. Frey, M. Koch, M. Koennecke, V. Pomjakushin, J. Schefer, R. Thut, N. Schlumpf, R. Buerge, U. Greuter, S. Bondt, and E. Berruyer, Physica B **276-278**, 146 (2000); [http://sinq.web.psi.ch/hrpt].
[38]J. Rodriguez-Carvajal, Physica B **192**, 55 (1993); [http://www.ill.eu/sites/fullprof/].
[39]Y. A. Izyumov, V. E. Naish, and R. P. Ozerov, *Neutron Diffraction of Magnetic Materials* (Consultants Bureau, New York, 1991).
[40]A. Zheludev, S. Maslov, G. Shirane, Y. Sasago, N. Koide, and K. Uchinokura, Phys. Rev. Lett. **78**, 4857 (1997).
[41]A. E. Jacobs and T. Nikuni, J. Phys.: Condens. Matter **10**, 6405 (1998).
[42]B. Roessli, J. Schefer, G. A. Petrakovskii, B. Ouladdiaf, M. Boehm, U. Staub, A. Vorotinov, and L. Bezmaternikh, Phys. Rev. Lett. **86**, 1885 (2001).